Journal of Materials Chemistry

Cite this: J. Mater. Chem., 2012, 22, 21443

www.rsc.org/materials

PAPER

Microcalorimetric insight into the analysis of the reactive adsorption of ammonia on Cu-MOF and its composite with graphite oxide†

Camille Petit,‡[a] Sabine Wrabetz[b] and Teresa J. Bandosz*[a]

Received 26th July 2012, Accepted 28th August 2012
DOI: 10.1039/c2jm34973f

The determination of reactive adsorption mechanisms on metal–organic frameworks remains largely unexplored and knowledge in that field would provide an important stepping stone in enhancing the performance of these materials for gas separation. In this study, the mechanisms of ammonia adsorption on HKUST-1 and its composite with graphite oxide (GO) were analyzed using microcalorimetry, and the results were compared to those derived from other characterization tools. The key to this study lies in conducting measurements at very low surface coverage in order to define the most energetic adsorption phenomena. It was found that ammonia reacted with the Cu sites and then with the ligands causing MOF to collapse. On the other hand, GO enhanced the heats of adsorption owing to its additional reactive sites.

Introduction

Over the past decade, extensive work in the field of materials science has been devoted to the study, characterization and analysis of the potential applications of metal–organic frameworks (MOFs).[1,2] They correspond to well-defined, semi-infinite networks consisting of metal ions or clusters (nodes) and organic ligands (struts).[1,2] Their tunable chemistry and morphology as well as their crystalline character and (typically) high porosity make them compelling candidates for applications involving gas separation, gas storage, chemical catalysis, drug delivery or molecular recognition.[3–6]

Although adsorption mechanisms in MOFs mostly involve physisorption, evidence of chemisorption when unsaturated metallic sites are present has been reported.[7–10] Besides physisorption and direct interaction with open metallic sites, it was shown that gas adsorption on some MOFs could also occur *via* reaction with the organic ligands (reactive adsorption), sometimes causing the destruction of the framework.[11–15] Chemisorption and reactive adsorption are crucial to the gas separation processes as they can enhance adsorption capacity and selectivity compared to the retention based only on physical adsorption. Nevertheless, the identification of the exact adsorption mechanisms on MOFs, other than physisorption, remains a challenge and additional knowledge on the nature of the adsorption sites and thermodynamics of adsorption is deemed necessary for the optimization of MOFs' adsorption properties. Measurements of heat of adsorption can help address such issues when used in conjunction with other analytical techniques. Recently, several studies have reported the heat of adsorption of different molecules on MOFs.[16–24] However, (i) most results only pointed toward the identification of physisorption mechanisms and (ii) data at very low surface coverage were often not determined. The latter could provide information on the most energetic/favorable adsorption sites.

In this paper, we report for the first time, to the best of our knowledge, the differential heats of adsorption of ammonia on HKUST-1 and its composite with GO from very low coverage up to $P/P_0 \sim 0.064$ (P_0: vapor pressure of adsorbate in the bulk state), with evidence of reactive adsorption. Comparison between HKUST-1 and its composite with GO is provided and linked to the differences in the adsorption phenomena. HKUST-1 was selected since it is known to chemically react with guest molecules owing to the presence of open metallic sites.[7] HKUST-1 is a representative MOF that consists of Cu(II) ions as paddlewheel-coordinated nodes and benzene tricarboxylates (BTC) as struts (Fig. 1(a and b)).[25] Besides the presence of unsaturated metallic sites, the relevant properties of HKUST-1 in the field of gas adsorption include its high porosity,[25] and its stability under humid conditions.[26] The purpose of building MOF/GO composites (herein referred to as HKUST-1/GO) as a new air filtration medium was to enhance the dispersive forces of MOFs *via* the addition of a material (GO) with the dense array of atoms.[11,27–29] Indeed, although MOFs exhibit attractive features for gas adsorption such as a high porosity and a well-developed chemistry, its "airy" nature and rather large pores result in weak

[a]*The Department of Chemistry, The City College of New York and the Graduate School of the City University of New York, 160 Convent Avenue, New York, USA. E-mail: tbandosz@ccny.cuny.edu; Fax: +1 212-650-6107; Tel: +1 212-650-6017*
[b]*Fritz-Haber-Institut der Max-Planck-Gesellschaft, Faradayweg 4-6, 14195 Berlin, Germany*

† Electronic supplementary information (ESI) available: Raw microcalorimetric data. See DOI: 10.1039/c2jm34973f

‡ Present address: The Departments of Chemical Engineering and Earth and Environmental Engineering, Columbia University, 500 West 120th street, New York, USA.

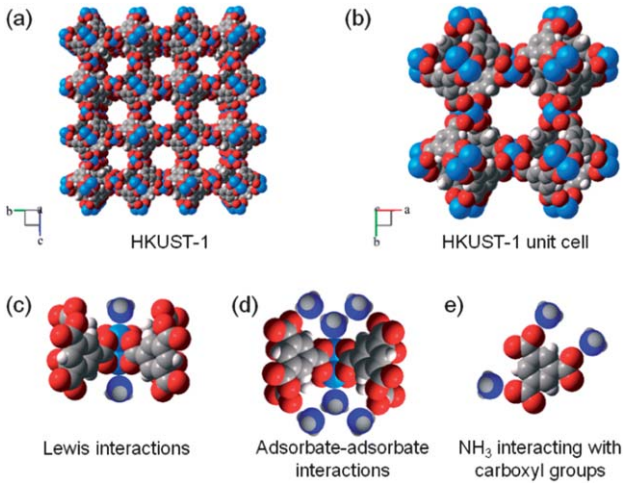

Fig. 1 (a and b) HKUST-1 structure and unit cell. (c–e) Mechanisms of ammonia adsorption on HKUST-1 with highlight on a $Cu_2(BTC)_4$ unit and its interactions with ammonia. Atoms: grey, carbon; light blue, copper; white, hydrogen; red, oxygen; dark blue, nitrogen. The HKUST-1 structure was plotted using Balls and Sticks software (T. C. Ozawa and S. J. Kang, *J. Appl. Crystallogr.*, 2004, **37**, 679). The CIF was created using the data provided in ref. 25.

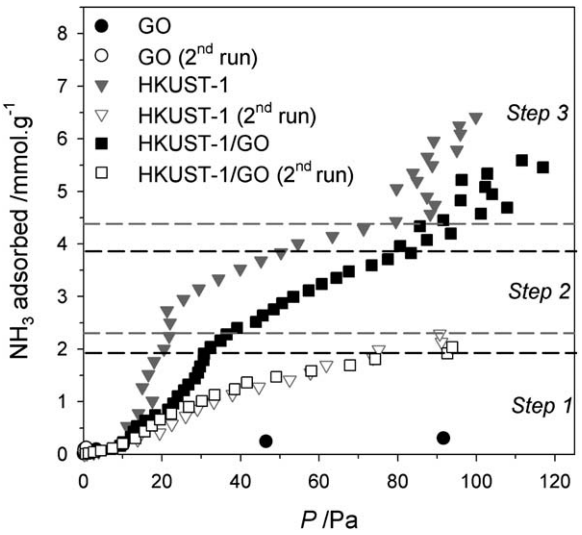

Fig. 2 NH_3 adsorption and re-adsorption isotherms at 313 K.

dispersive forces and thus impair the retention of small gas molecules. The results of previous work have demonstrated the positive impact of building MOF/GO composites in addressing this issue.[11,29] Briefly, the results showed that HKUST-1 had the expected structure. Moreover, GO in the composite was well-dispersed within the MOF units and coordinations existed between the oxygen groups of GO and the unsaturated metallic centers of HKUST-1. These bonds allowed the creation of a new pore space in the interface between the GO layers and the HKUST-1 units.[27] In this pore space, the dispersive forces were enhanced owing to the high atomic density of GO. The synergistic effect observed in gas adsorption using HKUST-1/GO compared to HKUST-1 was linked to this new pore space.[11]

Results and discussion

The isotherms of HKUST-1 and HKUST-1/GO, shown in Fig. 2, exhibit similar patterns, owing to the large HKUST-1 content in the composite. For both samples, the first adsorption isotherm consists of several steps that indicate the complexity of the adsorption process. Overall, three steps can be distinguished: (i) 0 to 2.0 mmol g^{-1} (0 to 1.9 mmol g^{-1} for the composite), (ii) 2.0 to 4.2 mmol g^{-1} (1.9 to 3.9 mmol g^{-1} for the composite) and, (iii) above 4.2 mmol g^{-1} (3.9 mmol g^{-1} for the composite). The final adsorption capacities (~6.0 mmol g^{-1} for HKUST-1 and ~5.4 mmol g^{-1} for the composite) are high compared to those measured on other adsorbents.[30] After the first adsorption run, the materials were outgassed at 393 K ($P \leq 10^{-10}$ Pa), and a second adsorption run was conducted. Compared to the first run, the amount of NH_3 adsorbed during re-adsorption on HKUST-1 and HKUST-1/GO significantly decreased (31–36% of the initial capacity). Although additional adsorption runs were not conducted in the interest of time, it is expected that once the most reactive sites are involved in surface reactions, the adsorption capacity would stabilize at the low level. Overall, this decrease of adsorption capacity in the second run clearly indicates that some of the adsorption sites are not recovered after the pressure/temperature swing. This may be caused by the irreversible collapse of the materials, as discussed later. Interestingly, there is no difference between the isotherms of HKUST-1 and HKUST-1/GO samples for the second adsorption run. This may be due to a larger decrease in the surface area as a result of the MOF collapse in the case of HKUST-1 compared to the composite. In fact, in a previous study conducted on similar materials, it was found that the porosity decrease was more pronounced in the case of HKUST-1 than that for the composite.[16] Surprisingly, GO adsorption capacity is low (below 0.4 mmol g^{-1}), although other studies under dynamic conditions reported good performance of the material for NH_3 removal owing to the reactions between NH_3 and the oxygen groups of GO.[31] This unexpected behavior may be due to the pretreatment conducted prior to the heat of adsorption measurement. Heating at elevated temperature and high vacuum outgassing likely caused the decomposition of the least stable functional groups of GO (*e.g.*, epoxy groups), and thus prevented their interactions with ammonia molecules.[31]

The analysis of the heat of adsorption (Fig. 3) can bring further details on the adsorption mechanisms reflected through the shape of the adsorption isotherms. The raw data of the integral heat signals are given in Fig. S1–S4 (HKUST-1: S1, S2 and HKUST-1/GO: S3, S4†). The differential heats of HKUST-1 and HKUST-1/GO are similar and the curves can be divided into the three sections described above for the adsorption isotherms. For HKUST-1, a plateau at 82 kJ mol^{-1} is first noticed (up to 2.0 mmol g^{-1}). From 2.0 to 4.2 mmol g^{-1}, the heat stabilizes at about 70 kJ mol^{-1} and finally, an erratic noisy pattern is observed above 4.2 mmol g^{-1}. This erratic pattern is likely associated with complex processes, indicative of secondary chemical reactions and the change in the porous structure of the adsorbents (collapse). Such reactive processes are evidenced by the presence of bumps in the heat integral curves of HKUST-1 in Fig. S2.† The trends in the heats of adsorption on HKUST-1/GO

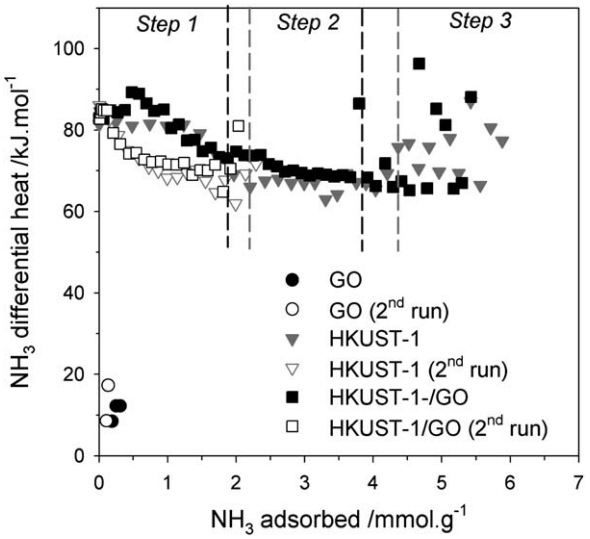

Fig. 3 Differential heats of adsorption of NH_3 at 313 K.

and HKUST-1 are alike. The only difference is the absence of a plateau on the curve for HKUST-1/GO at low coverage and the fact that secondary processes are observed in the range 0.4 mmol g^{-1} to 1.9 mmol g^{-1} (Fig. S4†). This was not the case for HKUST-1 (Fig. S1†). These differences must be linked to the presence of GO in the composite and potential explanation for this feature is discussed below. The heats measured during the re-adsorption run are almost identical for the two samples: the heat at zero coverage is about 90 kJ mol^{-1}, and is followed by a progressive decrease. Overall, the heats of ammonia adsorption measured on the two materials for both the first and second adsorption runs are considered high, thereby indicating chemical adsorption and/or reactive adsorption. The variability in the heat of adsorption with an increase in surface coverage and the detected secondary processes indicate the complexity of the adsorption processes. In contrast, the heat of adsorption measured on GO is rather small (<15 kJ mol^{-1}), which we link to the decomposition of oxygen groups during the pretreatment, as explained above. These groups were identified as reactive sites for ammonia.[31]

Taking into account the steps of adsorption described above, the trends in the heats of adsorption along with the findings of previous work using different analytical techniques,[11,27] we propose here to link this data to the mechanisms of adsorption taking place on HKUST-1 and HKUST-1/GO. During the first step of adsorption on HKUST-1 (0 to 2.0 mmol g^{-1}), NH_3 binds the Cu sites *via* Lewis acid–base interactions (Fig. 1(c)). This phenomenon is supported by the quick change of color of the material upon exposure to NH_3 (from dark blue to light blue).[11] Moreover, the high heat of adsorption is in good agreement with this chemisorption/reactive adsorption phenomenon. Interestingly, only half of the copper sites are occupied at the end of the heat plateau (HKUST-1 contains ~4.5 mmol g^{-1} Cu). This behavior can be explained by the fact that first, ammonia molecules must adsorb on the highest energy centers which are likely evenly distributed within the MOF cavities. Adsorption of ammonia on these specific Cu sites modifies/lowers the energy of the neighboring Cu sites leading to the decrease in the heat of adsorption. Thus these sites are occupied in the second step (2.0 to 4.2 mmol g^{-1}). This decrease in the adsorption energy of the second Cu site in the presence of ammonia can be linked to NH_3–NH_3 interactions/hydrogen bonds, which weaken the energy of the second copper site–NH_3 interactions. The presence of NH_3 in the pore space, as a result of the coordination with copper, and the addition of more NH_3 molecules involved in additional adsorbate–adsorbate interactions (Fig. 1(d)) likely create some tension/distortion within the MOF network. This causes the weakening and finally the breakage of some of the linkages between the Cu sites and the BTC ligands. This is evidenced in previous studies, in which the collapse of the MOF network was confirmed by several techniques: X-ray diffraction (XRD)[11] and porosity measurements indicated the reduced crystallinity and porosity,[16] while the release of the ligands was observed using FT-IR spectroscopy.[11] In particular, the surface areas of HKUST-1 (909 m^2 g^{-1}) and HKUST-1/GO (989 m^2 g^{-1}) decreased by about 86% and 82%, respectively after the first adsorption run. This leads to a decrease in the adsorbent effectiveness in subsequent adsorption runs as discussed above. As a result of this framework destruction, some of the ligands are released and then react with NH_3 (Fig. 1(e)). This is supported by thermogravimetric analyses run on the exhausted samples suggesting the formation of new complexes with carboxylic acids.[11] This reactive mechanism and the adsorbate–adsorbate interactions may occur simultaneously and are responsible for the scattering observed in the heat of adsorption above 4.2 mmol g^{-1}. They account for the secondary processes observed on the raw microcalorimetric data (Fig. S2†) and the second color change observed during the adsorption run.[11] The porosity and well-ordered structure of HKUST-1, both partially lost during the first adsorption run as shown by XRD and porosity analyses,[11,16] cannot be recovered during the subsequent heat/vacuum treatment. However, it is likely that NH_3 molecules involved in interactions with the organic ligands were desorbed considering the low thermal stability of carboxylate salts[32] and the previous results.[16] Therefore, during the re-adsorption, NH_3 could again react with the organic ligands leading to some sustained capacity at the low level. This is supported by the fact that the amount of NH_3 adsorbed during the second run (about 2 mmol g^{-1}) is similar to that measured during the last step of the first adsorption run (difference between 4.2 mmol g^{-1} and 6.0 mmol g^{-1}). The progressive decrease in the heat of adsorption during the re-adsorption must be due to the heterogeneous structure of the collapsed MOF: NH_3 first reacts with the ligands causing the partial expansion of the structure and then, ammonia can be physically adsorbed in created pores/cavities.

Adsorption on the composite must proceed following the same steps as those for HKUST-1 since its GO content is very low and the isotherms and heats of adsorption of the two samples are alike. However, the difference described above must be linked to the presence of GO. Particularly, the absence of a plateau in the heat of adsorption on the composite from 0 to 2.0 mmol g^{-1} and the evidence of secondary processes in that range (Fig. S4†) must be linked to the reactions of NH_3 with the GO oxygen groups *via* H-bonding (heat increase of about 10 kJ mol^{-1}). This adsorption mechanism occurs in addition to the Lewis interactions with the Cu sites.

Experimental section

Materials synthesis

GO was synthesized using the Hummers method,[28,31] in which commercial graphite powder (Sigma-Aldrich, 10 g) was stirred in concentrated sulfuric acid (230 mL, 273 K). Then, potassium permanganate (30 g) was slowly added to the suspension. The rate of addition was controlled to prevent the rapid rise in the temperature of the suspension (should be less than 293 K). The reaction mixture was then cooled to 275 K. After removal of the ice-bath, the mixture was stirred at room temperature for 30 min. Distilled water (230 mL) was slowly added to the reaction vessel, keeping the temperature less than 371 K. The diluted suspension was stirred for an additional 15 min and further diluted with distilled water (1.4 L) and then hydrogen peroxide (100 mL, 30 wt% solution) was added. The mixture was left overnight. GO particles settled at the bottom were separated from the excess liquid by decantation. The remaining suspension was transferred to dialysis tubes (MW cutoff 6000–9000). Dialysis was carried out until no precipitate of $BaSO_4$ was detected by addition of an aqueous solution of $BaCl_2$. Then, the wet form of graphite oxide was separated by centrifugation. The gel-like material was freeze-dried and a fine dark brown powder of the initial graphite oxide was obtained.

The synthesis of HKUST-1 was conducted as described in ref. 10, following a procedure adapted from Millward and coworkers' method.[33] Briefly, HKUST-1 was prepared by dissolving copper nitrate hemipentahydrate (10 g) and 1,3,5-benzenetricarboxylic acid (BTC, 5 g) in a mixture of *N*,*N*-dimethylformamide (85 mL), ethanol (85 mL) and deionized water (85 mL). The mixture was subjected to stirring and sonication to ensure complete dissolution of the crystals. The mixture was then heated at 358 K under shaking for about 20 h. After cooling, the crystals were filtered, washed and immersed in dichloromethane. Dichloromethane was changed twice during three days. Finally, the crystals were collected and dried under vacuum at 443 K for 28 h. The resulting product was kept in a desiccator and is referred to as HKUST-1.

HKUST-1/GO composites were prepared by dispersing GO powder in a well-dissolved copper nitrate–BTC mixture. The resulting suspension was then subjected to the same synthesis procedure as for HKUST-1, as described in ref. 27. The added GO consisted of about 5 wt% of the final material.

Microcalorimetric tests and adsorption isotherm measurements

The microcalorimetry measurements were conducted at 313 K on a SETARAM MS70 Calvet calorimeter combined with a custom-designed high vacuum and gas dosing apparatus, which was described in detail in ref. 34. The dosing volume was 139 mL, and an absolute pressure transducer (MKS Baratron type 121) was used to measure pressure variations of 0.3 Pa in this volume (provided the box temperature did not vary by more than 1.5 K), allowing (as a conservative estimate) to dose as low as 0.02 μmol into the sample cell. An all-metal cell was employed as described in ref. 35, but without the basket-like insert. The degassing of the samples was conducted inside the calorimeter cell but outside of the calorimeter using a separate turbomolecular pumping station. After evacuation at 393 K for 1.5 h to a pressure $\leq 10^{-10}$ Pa, the cell was closed and transferred into the calorimeter. Subsequently, NH_3 was introduced into the initially evacuated cell, and the pressure evolution and the heat signal were recorded for each dosing step. The adsorption isotherm was derived from the dosed amount and the equilibrium pressure (in comparison to an empty cell). The differential heats of adsorption were calculated by converting the signal area into heat using the calorimeter's calibration factor and then adjusting for the number of molecules adsorbed in this step. The desorption of NH_3 was performed by means of the turbomolecular pump at adsorption temperature at 393 K up to $\leq 10^{-10}$ Pa.

Conclusions

In conclusion, the microcalorimetric analysis of ammonia adsorption on HKUST-1 and its composite with GO highlights the chemisorption and reactive adsorption mechanisms (and their order of occurrence) taking place from the very low coverage stage up to $P/P_0 \sim 0.064$. The main mechanisms include the Lewis interactions of NH_3 and the Cu sites (70–80 kJ mol^{-1}) and the reaction of NH_3 with the ligands (70–100 kJ mol^{-1}). Overall this study demonstrates that microcalorimetry, especially at low coverage levels, in concert with other analytical tools can be used to identify adsorption mechanisms in MOFs and their thermodynamics. Other challenges in this field would be to use such techniques for a variety of MOFs and gases to unveil new adsorption processes in the materials and eventually tune the adsorbents for specific gas separation usages.

This work was supported at CCNY/CUNY by the Army Research Office grant W911NF-10-1-0030 and NSF Collaborative grant 0754945/0754979.

Notes and references

1 P. Wright, *Microporous Framework Solids*, RSC Publishing, Cambridge, UK, 2008.
2 S. L. James, *Chem. Soc. Rev.*, 2003, **32**, 276.
3 U. Müller, M. M. Schubert and O. M. Yaghi, in *Handbook of Heterogeneous Catalysis*, ed. G. Ertl, H. Knözinger, F. Schüth and J. Weitkamp, WILEY-VCH, Weinheim, 2008, vol. 1, pp. 247–262.
4 A. U. Czaja, N. Trukhan and U. Müller, *Chem. Soc. Rev.*, 2009, **38**, 1284.
5 P. Horcajada, C. Serre, M. Vallet-Regí, M. Sebban, F. Taulelle and G. Férey, *Angew. Chem., Int. Ed.*, 2006, **45**, 5974.
6 B. Chen, S. Xiang and G. Qian, *Acc. Chem. Res.*, 2010, **43**, 1115.
7 C. Prestipino, L. Regli, J. G. Vitillo, F. Bonino, A. Damin, C. Lamberti, A. Zecchina, P. L. Solari, K. O. Kongshaug and S. Bordiga, *Chem. Mater.*, 2006, **18**, 1337.
8 D. Britt, D. Tranchemontagne and O. M. Yaghi, *Proc. Natl. Acad. Sci. U. S. A.*, 2008, **105**, 11623.
9 B. Chen, X. Zhao, A. Putkham, K. Hong, E. B. Lobkovsky, E. J. Hurtado, A. J. Fletcher and K. M. Thomas, *J. Am. Chem. Soc.*, 2008, **130**, 6411.
10 J.-R. Li, R. J. Kuppler and H. C. Zhou, *Chem. Soc. Rev.*, 2009, **38**, 1477.
11 C. Petit, B. Mendoza and T. J. Bandosz, *Langmuir*, 2010, **26**, 15302.
12 B. Levasseur, C. Petit and T. J. Bandosz, *ACS Appl. Mater. Interfaces*, 2010, **2**, 3606.
13 C. Petit, B. Mendoza and T. J. Bandosz, *ChemPhysChem*, 2010, **11**, 3678.
14 A. Demessence, D. M. D'Alessandro, M. L. Foo and J. R. Lon, *J. Am. Chem. Soc.*, 2009, **131**, 8784.
15 J. J. Gassensmith, H. Furukawa, R. A. Smaldone, R. S. Forgan, Y. Y. Botros, O. M. Yaghi and J. F. Stoddart, *J. Am. Chem. Soc.*, 2011, **133**, 15312.

16 C. Petit, L. Huang, J. Jagiello, J. Kenvin, K. E. Gubbins and T. J. Bandosz, *Langmuir*, 2011, **27**, 13043.
17 Z. Bao, L. Yu, Q. Ren, X. Lu and S. Deng, *J. Colloid Interface Sci.*, 2011, **353**, 549.
18 D. Yuan, R. B. Getman, Z. Wei, R. Q. Snurr and H.-C. Zhou, *Chem. Commun.*, 2012, **48**, 3297.
19 L. Bastin, P. S. Barcia, E. J. Hurtado, J. A. C. Silva, A. E. Rodrigues and A. Chen, *J. Phys. Chem. C*, 2008, **112**, 1575.
20 Z. Zhang, S. Huang, S. Xian, H. Xi and Z. Li, *Energy Fuels*, 2011, **25**, 835.
21 D. Saha, Z. Wei and S. Deng, *Sep. Purif. Technol.*, 2009, **64**, 280.
22 S. Ma, D. Sun, J. M. Simmons, C. D. Collier, D. Yuan and H.-C. Zhou, *J. Am. Chem. Soc.*, 2007, **130**, 1012.
23 P. L. Llewellyn, S. Bourrelly, C. Serre, A. Vimont, M. Daturi, L. Hamon, G. De Weireld, J.-S. Chang, D.-Y. Hong, Y. Kyu Hwang, S. Hwa Jhung and G. Férey, *Langmuir*, 2008, **24**, 7245.
24 J. An, S. J. Geib and N. L. Rosi, *J. Am. Chem. Soc.*, 2009, **132**, 38.
25 S. S.-Y. Chui, S. M.-F. Lo, J. P. H. Charmant, A. G. Orpen and I. D. Williams, *Science*, 1999, **283**, 1148.
26 P. Küsgens, M. Rose, I. Senkovska, H. Fröde, A. Henschel, S. Siegle and S. Kaskel, *Microporous Mesoporous Mater.*, 2009, **120**, 325.
27 C. Petit, J. Burress and T. J. Bandosz, *Carbon*, 2011, **49**, 563.
28 C. Petit and T. J. Bandosz, *Adv. Mater.*, 2009, **21**, 4753.
29 C. Petit and T. J. Bandosz, *Adv. Funct. Mater.*, 2010, **20**, 111.
30 J. Helminen, J. Helenius, E. Paatero and I. Turunen, *J. Chem. Eng. Data*, 2001, **46**, 391.
31 C. Petit, S. Seredych and T. J. Bandosz, *J. Mater. Chem.*, 2009, **19**, 9176.
32 L. Erdey, S. Gál and G. Liptay, *Talanta*, 1964, **11**, 913.
33 A. R. Millward and O. M. Yaghi, *J. Am. Chem. Soc.*, 2005, **127**, 17998.
34 L. C. Jozefowicz, H. G. Karge and E. N. Coker, *J. Phys. Chem.*, 1994, **98**, 8053.
35 E. N. Coker and H. G. Karge, *Rev. Sci. Instrum.*, 1997, **68**, 4521.